separations

MDPI

Article

Estimation of Bed Expansion and Separation Density of Gas–Solid Separation Fluidized Beds Using a Micron-Sized-Particle-Dense Medium

Xuchen Fan [1,2,*] and Chenyang Zhou [1,2,*]

[1] Key Laboratory of Coal Processing & Efficient Utilization, Ministry of Education, China University of Mining & Technology, Xuzhou 221116, China
[2] School of Chemical Engineering & Technology, China University of Mining & Technology, Xuzhou 221116, China
* Correspondence: cumtfxc@cumt.edu.cn (X.F.); zhoucy@cumt.edu.cn (C.Z.)

Abstract: Coal is the dominant energy resource in China. With the Chinese policy of committing to reducing peak carbon dioxide emissions and achieving carbon neutrality, coal separation has recently become a hot topic, especially the fluidized separation of fine particles. In this study, micron-sized particles were introduced to ameliorate the properties of the traditional fluidized bed. The expansion characteristics of the micron-sized-particle-dense medium were explored. A bed expansion prediction model of the micron-sized-particle-dense medium was established, and the prediction error was about 10%, providing a theoretical basis for understanding the distribution characteristics of the bed. This model also helped predict the bed density in the presence of a micron-sized-particle-dense medium, and the prediction accuracy was between 85% and 92%, providing a theoretical basis for selecting and popularizing fluidized beds for industrial separation.

Keywords: two-phase theory; micron-sized particles; bed height; fluidized bed; bubble phase; emulsion phase; bed expansion; bed density

Citation: Fan, X.; Zhou, C. Estimation of Bed Expansion and Separation Density of Gas–Solid Separation Fluidized Beds Using a Micron-Sized-Particle-Dense Medium. *Separations* **2021**, *8*, 242. https://doi.org/10.3390/separations8120242

Academic Editor: Fen Jiao

Received: 4 November 2021
Accepted: 9 December 2021
Published: 10 December 2021

1. Introduction

With the Chinese policy of committing to reducing peak carbon dioxide emissions and achieving carbon neutrality, coal separation has recently become a hot topic, especially the gas–solid fluidized separation technology [1–3]. Therefore, the clean and efficient use of coal has attracted researchers' attention in various countries [4–8]. In general, wet methods are adopted for the clean utilization of coal, such as jigging [9], heavy medium cyclones [10,11], TBS [12,13], and flotation [14]. However, it is difficult to carry out wet coal separation in northwest China due to the shortage of water resources [15]. Therefore, dry separation is the only way to achieve a clean and efficient use of coal. The typical dry separation methods include the use of air-dense medium fluidized beds [16–18], compound dry separators [19,20], and air jigs [21,22]. These methods are commonly used to process coal above 6 mm and have achieved very significant separation results. With the development of coal processing technology, coal with a smaller particle size is produced, and more efficient methods are needed to effectively separate coal of less than 6 mm. The general practice is to introduce external forces into the traditional gas–solid fluidized bed, such as in vibrated fluidized bed [23–25], magnetically stabilized fluidized bed [26], and pulsating fluidized bed [27,28]. Although these methods play improve the separation effect, they involve increased energy consumption. Therefore, it is very important to find a more efficient method for fine coal separation. The traditional fluidized separation technology is effective for fine particle separation. In the carbon neutralization policy, energy conservation and emission reduction are very important. Compared with the wet coal separation method, the traditional fine-particle fluidized separation technology does not need extra water. Water will consume energy in the process of transportation and

circulation, resulting in an increase in carbon emissions. Compared with other external-force fluidized beds, the traditional fine-particle fluidized separation technology does not need too much extra energy; since energy consumption means an increase in carbon emissions, it is not conducive to the implementation of the carbon neutralization policy. Furthermore, the industrial modular fluidized bed process has been improved, limiting the system's dimensions and achieving its rapid construction, which can also reduce carbon emissions [29]. Therefore, the traditional fine-particle fluidized separation technology could help achieve carbon neutrality.

In a traditional gas–solid fluidized bed, a Geldart B particle-dense [30] medium (0.1–0.4 mm) is generally used as the dense medium for separation; however, Geldart B particles have some limitations [31]. First of all, the emulsion phase of a fluidized bed with Geldart B particles expands less during the process of separation, and the adjustment of emulsification relative to the fluidized bed density plays a crucial role [32]. Secondly, when the fluidized state is reached, the energy input required for the fluidized bed with Geldart B particle is large, resulting in increased energy consumption [33]. Finally, the internal stability of the fluidized bed with Geldart B particles is poor, and bubble movement is irregular [34]. Furthermore, the height of traditional fluidized beds is lower than 30 mm, which means there is not enough space for the expansion of the emulsion phase [35–37]. Therefore, the separation efficiency can be further improved.

In recent years, researchers have found that the introduction of fine particles in the fluidized bed can effectively improve the proportion of emulsion phase in the bed and enhance the stability of fluidization [38–40]. Matheson et al. focused on the influence of fine particles and analyzed the improvement of viscosity depending on the content of fine particles [38]. Bertil compared the minimum fluidization velocity of narrow particles and wide particles. It was found that increasing the particle size helps to reduce the minimum fluidization velocity of the particles [39].

In this study, in order to ameliorate fluidization and improve the separation efficiency, micron-sized particles (0.045–0.1 mm) were introduced. The expansion characteristics of the emulsion phase and bubble phase were studied. Combined with the two-phase theory of gas–solid fluidized beds, a bed expansion prediction model of the micron-sized-particle-dense medium was established, which provides a theoretical basis for understanding the distribution characteristics of the bed. Based on the bed expansion prediction model, the bed density was studied, providing a theoretical basis for selecting and popularizing fluidized beds for industrial separation.

2. Experimental

2.1. Apparatus

Figure 1 shows the schematic of the laboratory-scale fluidized bed system. The fluidized bed Plexiglas column had a 15.2 cm internal diameter (ID) and was 70 cm high. During the fluidization process, the bubble phase and emulsion phase are the main components of the fluidized bed. Bed height expansion is directly related to the above phases. Thus, accurate monitoring of bed height variation is crucial in the analysis of the distribution of the two phases. The bed height variation was recorded by a digital camera (Nikon D3200) with 25 frames in front of the fluidized bed on the same side of the two lights.

2.2. Dense Medium

Magnetite powder was used as the representative particles in the present study. The properties of the micron-sized particles are shown in Figure 2. The particles' was between 45 μm and 100 μm. The particles had a true density of 4.60 g/cm^3 and a bulk density of 2.54 g/cm^3.

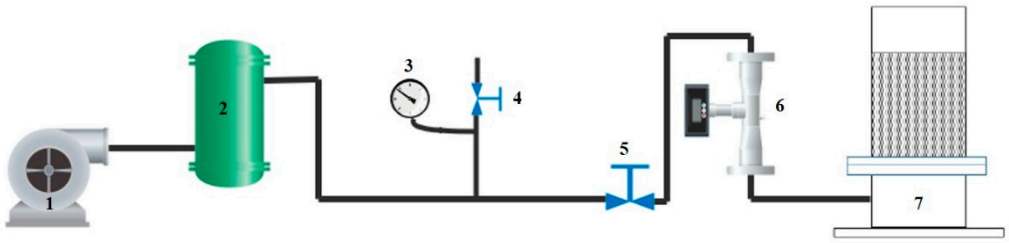

Figure 1. Scheme of the 3D gas–solid fluidized bed experimental system: (1) Blower; (2) Buffer tank; (3) Pressure gauge; (4) Valve; (5) Valve; (6) Flowmeter; (7) Fluidized bed.

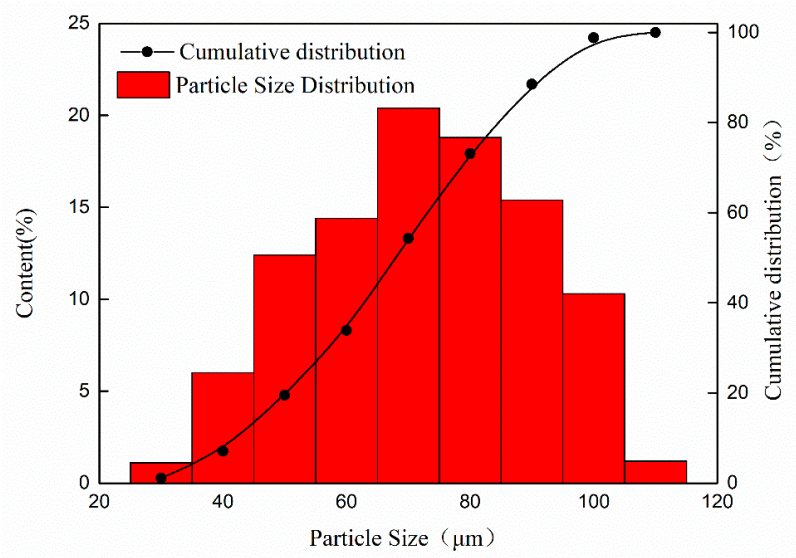

Figure 2. Particle size distribution of the micron-sized-particle-dense medium.

2.3. Feeding Particles' Properties

In this study, coal particles were selected as feeding particles. The washability curves of the feeding coal particles with size between −6 and + 3 mm are shown in Figure 3. As shown in Figure 3, the ash content of the coal particles was 29.59%, and the feeding coal particles were classified as middle-difficult-to-wash coal.

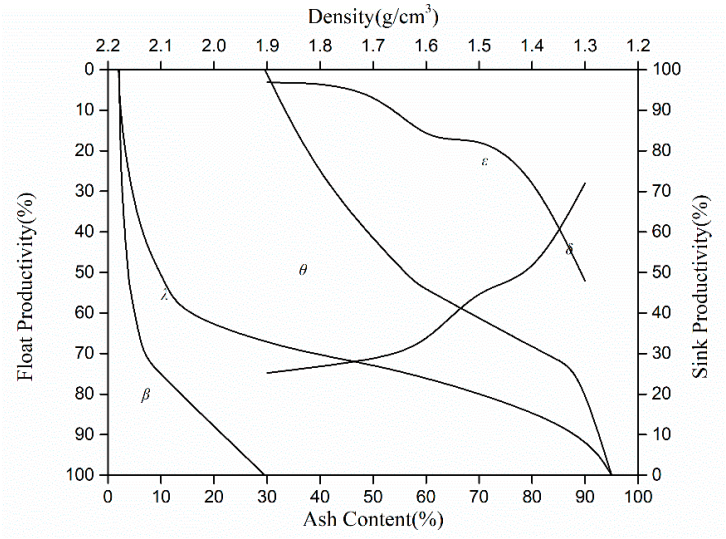

Figure 3. Washability curves of the feeding coal particles with size between −6 and + 3 mm.

3. Theoretic Analysis

3.1. Two-Phase Theory

In the gas–solid separation fluidized bed, the study of the two-phase distribution is helpful to analyze the distribution of the bubble phase and of the emulsion phase. Figure 4 shows the bubble phase and emulsion phase distribution based on the two-phase theory. It allowed the bed density prediction. For the gas–solid fluidized bed, Toomey and Jonestone proposed the first hypothesis of the two-phase theory [41]. Generally, when the fluidized bed enters the bubbling fluidization stage, the superficial gas velocity exceeds the minimum fluidization superficial gas velocity, thus producing bubbles, and the emulsion phase and the bubble phase coexist in the bed. Therefore, according to the two-phase theory in a bubbling fluidized bed, the gas passing through the bed is mainly the gas flowing out of the fluidized bed in the form of bubbles. The flow rate of the bubbles can be expressed by Equation (1):

$$Q_b = (U - U_{mf})A \tag{1}$$

where Q_b represents the flow rate of the surplus gas merged into the bubbles, in m^3/h; U represents the superficial gas velocity in the gas–solid fluidized bed, in cm/s; U_{mf} represents the minimum fluidization superficial gas velocity, in m/s, A represents the fluidized bed section area, in m^2.

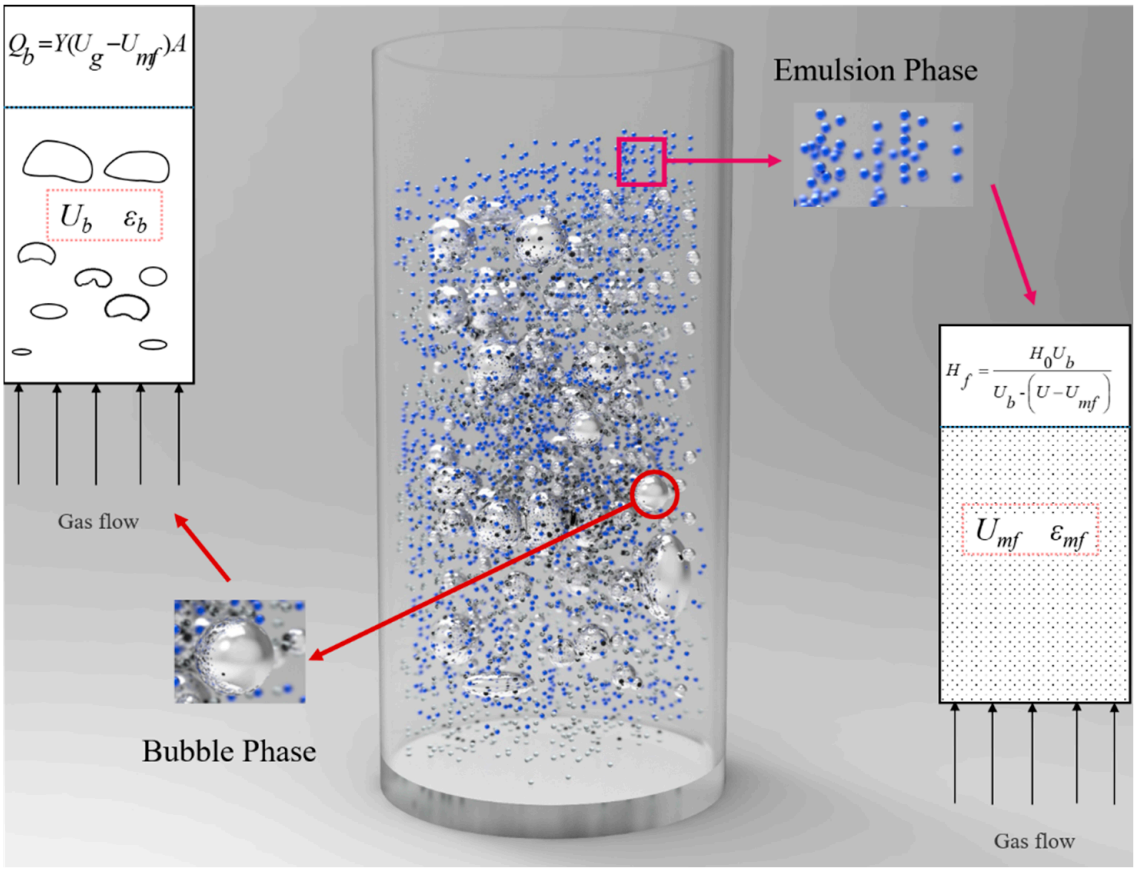

Figure 4. Schematic diagram of the original two-phase theory.

Because the above-mentioned two-phase theory overestimates the total volume of the bubble phase, scholars modified the two-phase theoretical model and proposed the introduction of a correction coefficient Y to correct the excess gas flow, as shown by Equation (2):

$$Q_b = Y(U_g - U_{mf})A \tag{2}$$

Y is the coefficient value in the Y-type two-phase theory and is about 0.8–0.85 for micron-sized particles [42,43].

3.2. Bed Expansion Prediction

Assuming that the velocity of the bubble at a certain bed height is U_b, the ratio of the bubble phase at a specific position can be expressed by Equation (3):

$$\varepsilon_b' = \frac{Q_b}{AU_b} \tag{3}$$

where ε_b' represents the bubble % phase content of a specific bed height.

Combined with Equations (2) and (3), the expansion rate caused by the bubble phase of the bed can be expressed by Equation (4):

$$\varepsilon_b = \frac{H_f - H_0}{H_f} = Y\frac{U - U_{mf}}{U_b} \tag{4}$$

The movement velocity of the bubbles in the fluidized bed of fine-grained particles can be expressed by Equation (5) [44]:

$$U_b = (U - U_{mf}) + 0.71(gd_b)^{1/2} \tag{5}$$

The bubble size can be expressed by Equation (6) [45]:

$$d_b = 0.54g^{-0.2}\left(U - U_{mf}\right)^{0.4}\left(h + 4{A_D}^{0.5}\right)^{0.8} \tag{6}$$

where h represents the position of the bubble, in m, and AD represents the area of the small holes on the gas distributor, in m^2.

In sum, the bed height could be estimated on the basis of the operating superficial gas velocity; the bed height is expressed by Equation (7):

$$H_f = \frac{H_0U_b}{U_b - Y\left(U - U_{mf}\right)} \tag{7}$$

4. Results and Discussions

4.1. Emulsion Phase Characterization in the Fluidized Bed

The emulsion phase expansion and the overall bed expansion height were analyzed. The expansion rate of the emulsion phase was selected as the evaluation index, and the expansion characteristics of micron-sized particles were studied to establish the law describing the emulsion phase expansion of micron-sized particles, as shown by Equation (8):

$$\varphi_d = H_d/H_0 \tag{8}$$

where φ_d is the expansion rate of the emulsion phase, H_0 is the initial bed height, in m, H_d is the bed height of the emulsion phase expansion, in m.

Figure 5 shows the effect of superficial gas velocity on the expansion rate of the emulsion phase. As the superficial gas velocity increased, the expansion rate of the emulsion phase first increased and then gradually stabilized and slightly decreased. With the further increase of the superficial gas velocity, the expansion rate of the emulsion phase remained unchanged and tended to a stable state. It can be noted that when the bed superficial gas velocity gradually increased to 1.82 cm/s, the overall expansion rate of the emulsion phase showed a slight downward trend, but the degree of reduction was relatively low. This was mainly because the micron-sized-particle-dense medium was also aerated. As the superficial gas velocity increased, the bed first showed a uniform emulsion phase expansion. At this stage, the emulsion phase expansion and the superficial gas velocity

showed a positive linear relationship. Therefore, when the superficial gas velocity was low, the particles in the fluidized bed were not fully expanded, and the bed expansion rate was low. As the superficial gas velocity continued to increase, bubbles began to appear in the bed, the bed entered the bubbling fluidization stage, and the expansion of the emulsion phase reached the upper limit. The expansion rate of the emulsion phase at this stage tended to stabilize. It should be pointed out that when the superficial gas velocity further increased, the proportion of the bubble phase continued to increase, which caused some of the gas in the emulsion phase to enter the bubbles. The increase of the bubble proportion reduced the expansion rate of the emulsion phase to a certain extent. Therefore, in the actual working process, the maximum superficial gas velocity should be controlled at $U < 1.82$ cm/s to ensure the full expansion of the emulsion phase of the bed.

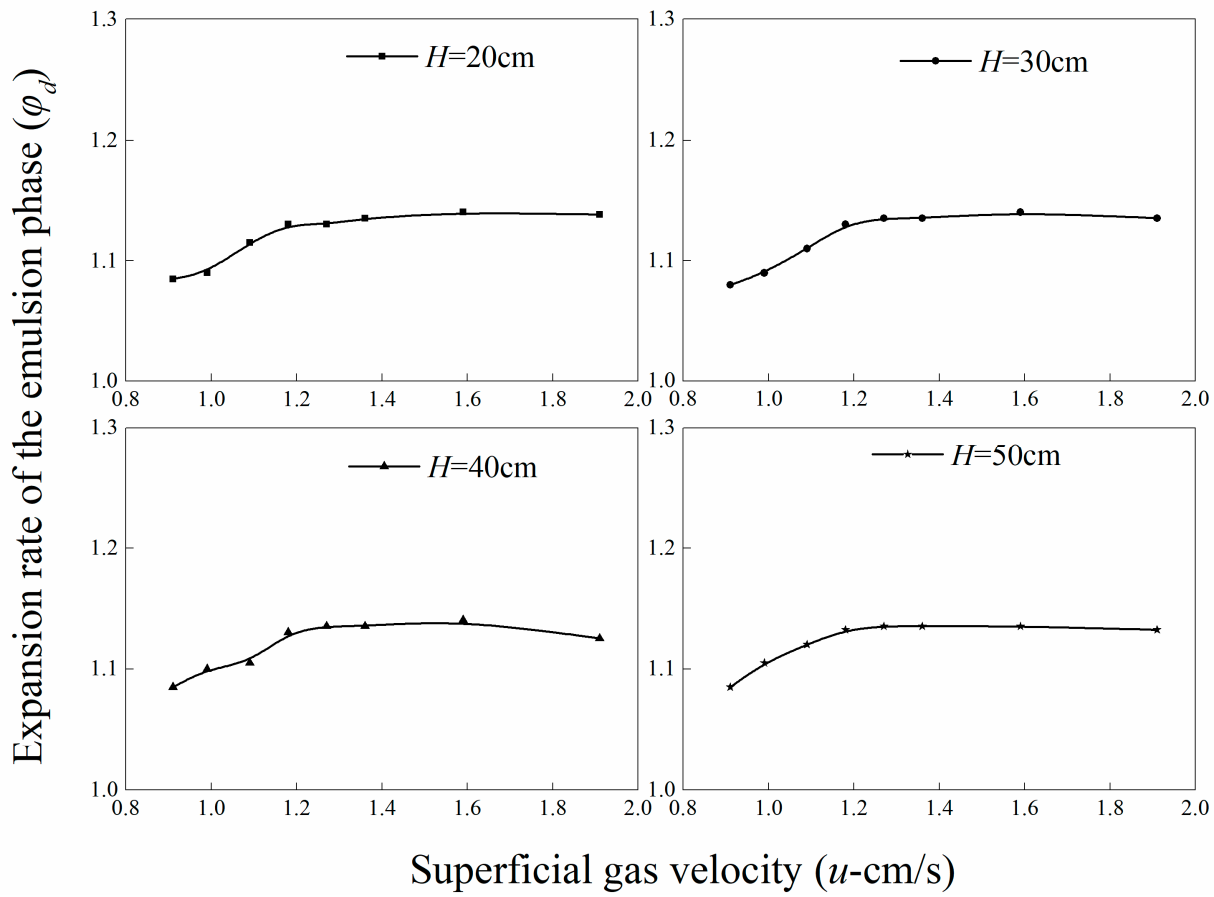

Figure 5. Effect of superficial gas velocity on the expansion of the emulsion phase.

In addition to the influence of the above-mentioned superficial gas velocity on the expansion behavior of the emulsion phase, we studied the effect of the bed height on the expansion rate of the emulsion phase. We selected the operating superficial gas velocity U = 1.17~1.59 cm/s to ensure the full bed expansion of the emulsion phase in the bed and better analyze the influence of the bed height on the expansion rate of the emulsion phase. Figure 6 shows the effect of the bed height on the expansion rate of the emulsion phase. With the increase of the bed height, the expansion rate of the emulsion phase decreased to a small extent and gradually stabilized for magnetite powder particles. With the gradual increase in bed height, the expansion rate of the emulsion phase tended to be stable. This indicated that for micron-sized particles, the bed height plays a dominant role in the expansion rate of the emulsion phase. When the bed height was low, the bubble size was smaller, and the bubble merging frequency was lower, which could provide sufficient conditions for the expansion of the particles. When the bed height gradually increased, the bubble merging frequency gradually increased as the bubbles rose, and the size of the

bubble was larger. The exchange rate between the gas in the emulsion phase and the gas in the bubble increased, which reduced the gas content in the emulsion phase to a certain extent and inhibited the full expansion of the emulsion phase. On the other hand, when the bed height increased further, the bubble behavior tended to be stable, the bubble size no longer increased, and the overall fluidization behavior of the bed tended to stabilize. Furthermore, the expansion rate of the emulsion phase tended to be stable. This is very advantageous for a gas–solid separation fluidized bed, as increasing the separation bed height increases the mineral separation capacity.

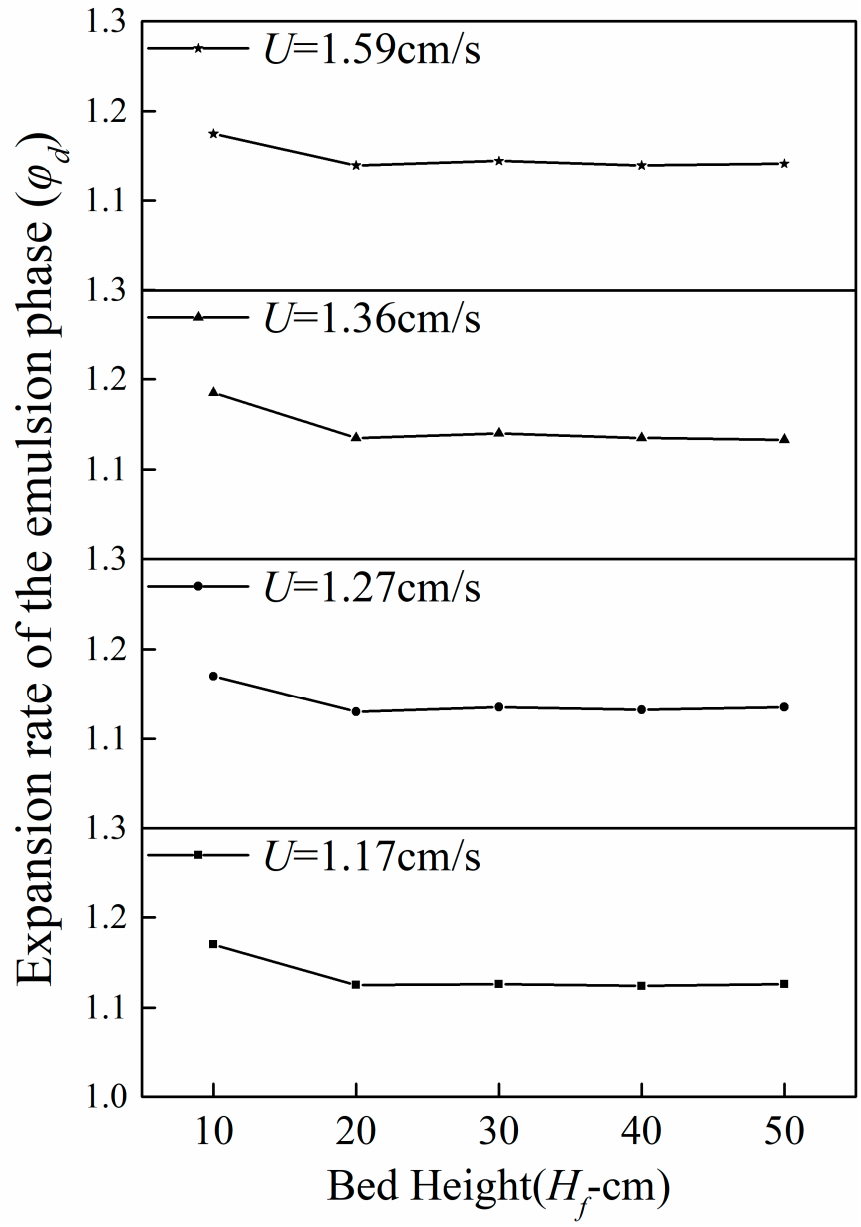

Figure 6. Effect of bed height on the expansion of the emulsion phase.

4.2. Bubble Phase Characterization in the Fluidized Bed

The gas–solid separation fluidized bed mainly contains two parts: the emulsion phase and the bubble phase. The emulsion phase is composed of particles and of the gas that fluidizes them, and the bubble phase is composed of the extra gas in the bed. Moreover, the bubbles continue to merge during the ascending process to form larger bubbles and flow out of the bed. Therefore, the expansion of the bed mainly involves the expansion of the emulsion phase and is caused by the movement of the bubble phase. The expansion

rate of the bubble phase can be obtained by the difference between the total expansion rate of the bed and the expansion rate of the emulsion phase. It helps to analyze the law governing the change of the bubble phase and facilitates the understanding of both the emulsion phase and the bubble phase.

The distribution ratio of the bubble phase ε_b in the fluidized bed can be expressed by Equation (9):

$$\varepsilon_b = 1 - \frac{H_d}{H_f} = \frac{H_b}{H_f} \tag{9}$$

where H_f is the total height of the expansion of the bed, in m; H_d is the expansion of the emulsion phase in the bed, in m; H_b is the expansion of the bubble phase, in m. The total height of bed expansion can be expressed by Equation (10):

$$H_f = H_d + H_b \tag{10}$$

Figure 7 shows the effect of superficial gas velocity on the bubble phase composition. With the gradual increase of the superficial gas velocity, the proportion of the bubble phase showed an increasing linear trend as a whole. This was mainly because when the superficial gas velocity was low, the gas in the bed was mainly used for the expansion of the emulsion phase, and the bubble content was low. When the superficial gas velocity gradually increased, the probability that the excess gas in the bed merged into bubbles increased, and the composition of the bubbles showed an increasing trend. The size of the bubble phase was larger, which caused an increase of the gas exchange frequency between the emulsion phase and the bubble phase. The gas entered the bubble phase more easily and flowed out of the bed in the form of bubbles, increasing the composition ratio of the bubble phase. Therefore, in the actual separation process, it was necessary to facilitate the control of the size of the bubbles and achieve a stable and efficient separation of minerals in the bed with the full expansion of the emulsion phase at an appropriate range of superficial gas velocity.

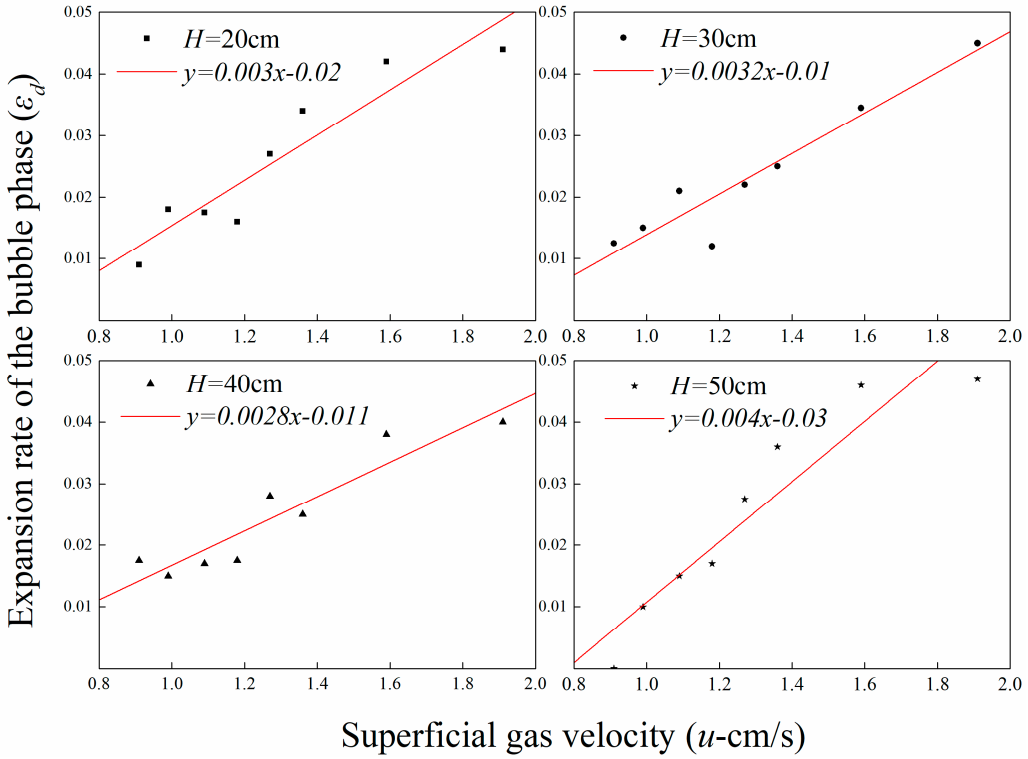

Figure 7. Effect of superficial gas velocity on the expansion of the bubble phase.

Figure 8 shows the effect of the bed height on the bubble phase composition for an operating superficial gas velocity U = 1.17~1.59 cm/s. The increase of the initial bed height had a lower influence on the bubble phase. The expansion rate showed a stable trend with a small overall degree of change. This was mainly because the bubbles changed less in the ascending process during the fluidization of micron-sized magnetite powder, and the bubble movement was stable. It further showed that the bubble behavior in the fluidized bed of micron-sized magnetite powder was relatively stable; in particular, when the bed height exceeded 30 cm, the bubble behavior became more stable. The bed expansion presented a more stable state which helped to provide a theoretical basis for the increase in the bed height and the enlargement of the fluidized separator.

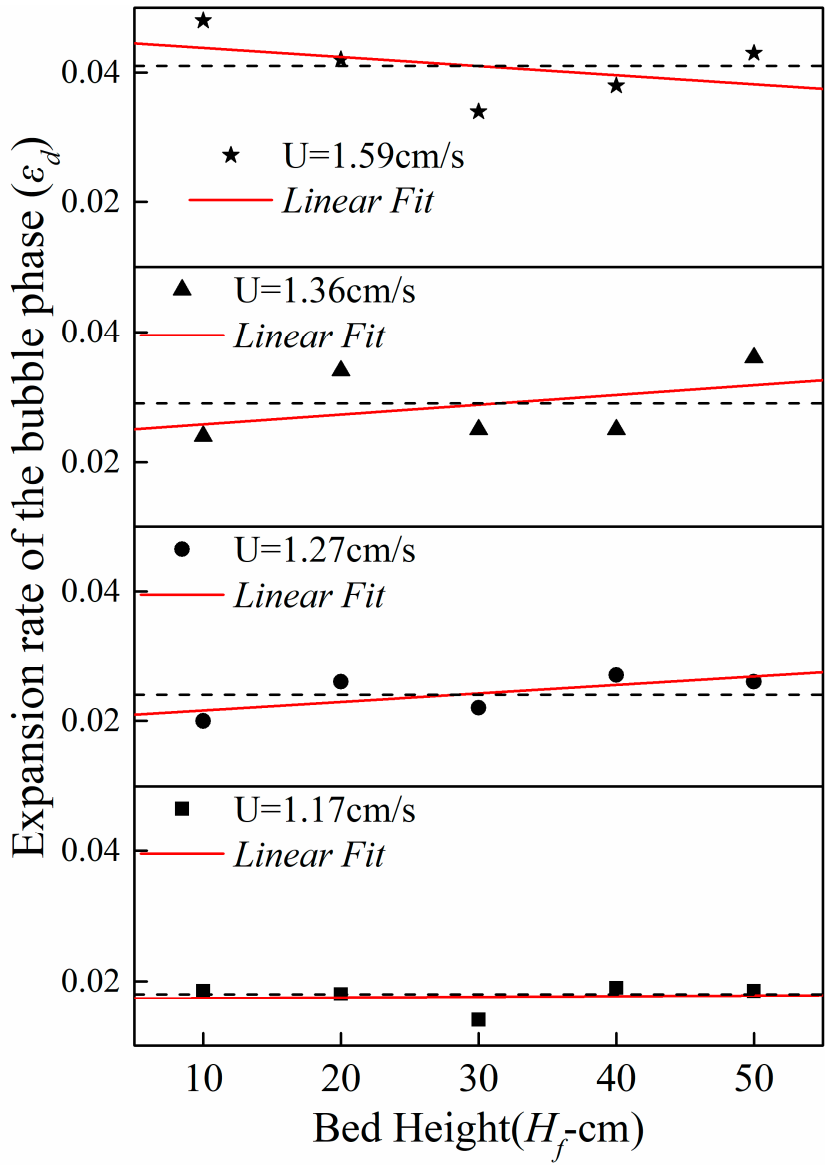

Figure 8. Effect of the bed height on the expansion of the bubble phase.

Therefore, the expansion of the bed height of a micron-sized-particle-dense medium separation fluidized bed can be calculated by Equations (7)–(9).

Considering the above theoretical research, and based on the above micron-sized magnetite powder research, the predicted bed expansion heights were compared with the experimental data when the initial bed height was H_0 = 10~50 cm and the operating superficial gas velocity was U = 0.90~1.82 cm/s.

Equation (7) was used to predict the expanded height of the bed and compare the difference between the theoretical calculation value and the experimental value. The corresponding error analysis was carried out to explore the applicability of the two-phase theory for a micron-sized-particle-dense medium. Figure 9 shows the comparison between the experimental value and the theoretical value of the bed expansion height. The error when using the two-phase theoretical model to predict the bed height was about 10%, indicating high reliability. However, the experiment results showed that the predicted value of the bed expansion height of micron-sized particles based on the two-phase theory was smaller than the actual value of the bed expansion height because the two-phase theory underestimated the expansion rate of the emulsion phase. This indicates that the existing two-phase theory of micron-sized particles still has certain shortcomings.

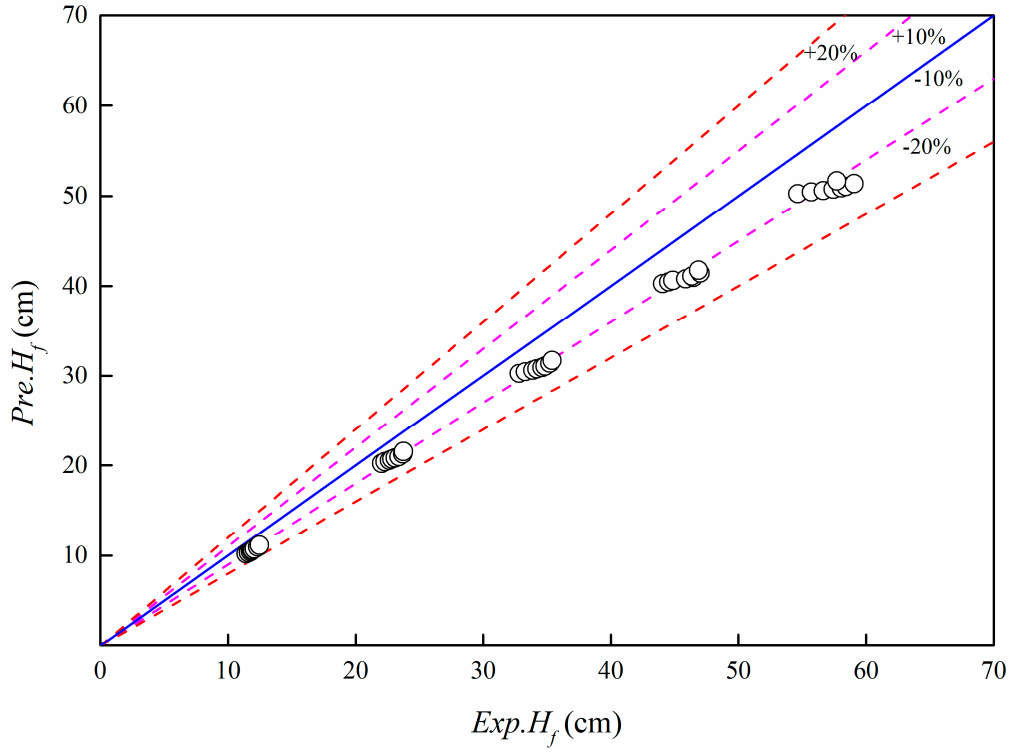

Figure 9. Error analysis of the predicting model of bed expansion of the micron-sized particle.

4.3. Bed Density

Bed density is important for fluidized bed separation, and the accuracy of the separation density is crucial to achieve separation. The fluidized bed separation process based on bed density is shown in Figure 10. When coal particles are fed into a fluidized bed, coal separation is based on the Archimedes principle. Light particles ($\rho_p < \rho_{bed}$) will rise, and heavy particles ($\rho_p > \rho_{bed}$) will fall. The bed density is the key to determine the position of the coal particles. It also has a dominant effect on coal separation. According to the bed expansion height, the bed density was predicted, the difference between the theoretical prediction value and the experimental value was determined, and the corresponding error analysis was carried out to explore the applicability of the two-phase theory in a micron-sized-particle-dense medium. The bed density can be expressed by Equation (11):

$$\begin{cases} \rho_{bed,EXP} = \frac{\Delta P}{gH_{f,EXP}} \\ \rho_{bed,PRE} = \frac{\Delta P}{gH_{f,PRE}} \end{cases} \quad (11)$$

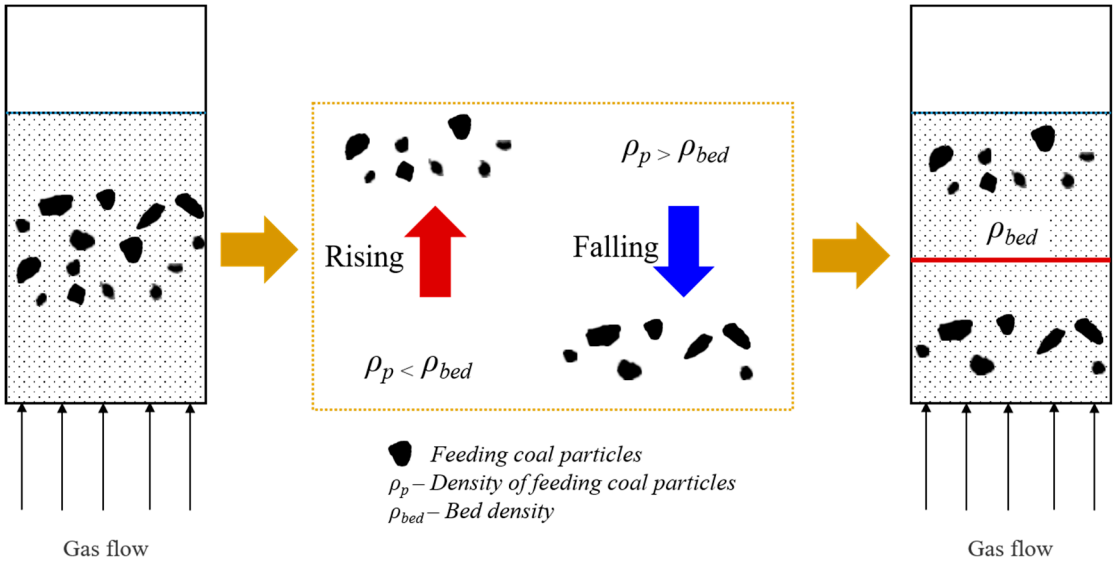

Figure 10. Fluidized bed separation process based on bed density.

Figure 11 shows the comparison between the experimental and the theoretical values of bed density. The error in predicting bed density by using the bed expansion prediction model was between 8 and15%, showing has high reliability and good prediction of the bed density. This provides a theoretical basis for the application of the gas–solid fluidized bed two-phase theory to a micron-sized-particle-dense medium. It also provides a theoretical basis for the further prediction of the separation density of feeding particles and for the application of micron-sized-particle-dense media in gas–solid separation fluidized beds.

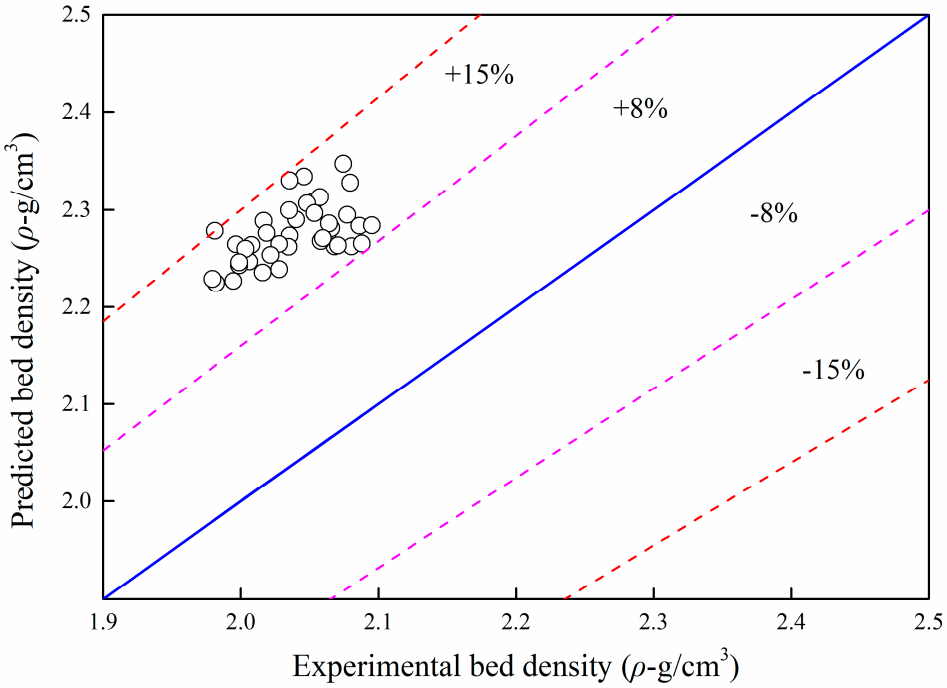

Figure 11. Error analysis in predicting the bed density of micron-sized particle.

5. Conclusions

In this study, the expansion characteristics of a micron-sized-particle-dense medium were explored, and the changes of the emulsion and bubble phases based on the operating parameters were analyzed:

(1) when the superficial gas velocity increased, the expansion rate of the emulsion phase first increased and then gradually stabilized and slightly decreased. With the increase of the bed height, the expansion rate of the emulsion phase decreased to a small extent and gradually stabilized;
(2) With the increase of superficial gas velocity, the proportion of the bubble phase showed an increasing trend as a whole, while the initial bed height had a little influence on the bubble phase.

Combined with the two-phase theory of gas–solid fluidized bed, a bed expansion prediction model of the micron-sized-particle-dense medium was established, and its prediction accuracy was between 85% and 92%. This model provides a theoretical basis for understanding the distribution characteristics of the bed and helps to simply predict the bed density that is suitable for a micron-sized-particle-dense medium. It also provides a theoretical basis for the selection and popularization of fluidized beds for industrial separation.

Author Contributions: Conceptualization, X.F. and C.Z.; methodology, X.F. and C.Z.; software, X.F. and C.Z.; validation, X.F. and C.Z.; formal analysis, X.F. and C.Z.; investigation, X.F. and C.Z.; resources, X.F. and C.Z.; data curation, X.F. and C.Z.; writing—original draft preparation, X.F. and C.Z.; writing—review and editing, X.F. and C.Z.; visualization, X.F. and C.Z.; supervision, X.F. and C.Z.; project administration, X.F. and C.Z.; funding acquisition, X.F. and C.Z. All authors have read and agreed to the published version of the manuscript.

Funding: This research was funded by the Fundamental Research Funds for the Central Universities, grant number 2018BSCXB14, and Postgraduate Research & Practice Innovation Program of Jiangsu Province, grant number KYCX18_1940.

Institutional Review Board Statement: Not applicable.

Informed Consent Statement: Not applicable.

Data Availability Statement: We have no intention to provide open data for the time being.

Acknowledgments: The authors wish to thank the China University of Mining and Technology and Jiangsu Province, CN for funding support.

Conflicts of Interest: The authors declare no conflict of interest.

References

1. Li, Z.; Hou, Y.; Cao, J.; Ding, Y.; Yuan, X. What drives green development in China: Public pressure or the willingness of local government? *Environ. Sci. Pollut. Res.* **2021**. [CrossRef]
2. Xie, Y.; Hou, Z.; Liu, H.; Cao, C.; Qi, J. The sustainability assessment of CO_2 capture, utilization and storage (CCUS) and the conversion of cropland to forestland program (CCFP) in the Water-Energy-Food (WEF) framework towards China's carbon neutrality by 2060. *Environ. Earth Sci.* **2021**, *80*, 468. [CrossRef]
3. Zhong, S.; Xin, C.; Shen, H.; Chen, X. Effects of land urbanization and internet penetration on environmental sustainability: A cross-regional study of China. *Environ. Sci. Pollut. Res.* **2021**, *28*, 66751–66771. [CrossRef] [PubMed]
4. Fan, X.; Zhang, G.; Zhao, Y.; Zhou, C.; Dong, L.; Duan, C. Effect of middling coal on separation efficiency in air dense gas–solid fluidized bed. *Int. J. Coal Prep. Util.* **2021**, *41*, 628–644. [CrossRef]
5. Asghari, M.; Noaparast, M.; Shafaie, S.Z.; Ghassa, S.; Chelgani, S.C. Recovery of coal particles from a tailing dam for environmental protection and economical beneficiations. *Int. J. Coal Sci. Technol.* **2018**, *5*, 253–263. [CrossRef]
6. Sahoo, S.K.; Suresh, N.; Varma, A.K. Determining the Best Particle Size-Class for Flotation of a High Ash Coal. *Int. J. Coal Prep. Util.* **2017**, *11*, 755–765. [CrossRef]
7. Saini, M.K.; Srivastava, P.K. Effect of Coal Cleaning on Ash Composition and its Fusion Characteristics for a High-Ash Non-Coking Coal of India. *Coal Prep.* **2017**, *37*, 1–11. [CrossRef]
8. Zhou, E.; Zhang, Y.; Zhao, Y.; Luo, Z.; Duan, C.; Yang, X.; Dong, L.; Zhang, B. Collaborative optimization of vibration and gas flow on fluidization quality and fine coal segregation in a vibrated dense medium fluidized bed. *Powder Technol.* **2017**, *322*, 497–509. [CrossRef]
9. Youqun, S.; Guilin, L.; Li, W. Research on the intelligent jigging coal separation calculation frame based on multi-agent. In Proceedings of the 2002 International Conference on Control and Automation, 2002. ICCA. Final Program and Book of Abstracts, Xiamen, China, 19 June 2002; p. 249.

10. Wang, B.; Chu, K.W.; Yu, A.B.; Vince, A. Modeling the Multiphase Flow in a Dense Medium Cyclone. *Ind. Eng. Chem. Res.* **2009**, *48*, 3628–3639. [CrossRef]
11. Chu, K.W.; Kuang, S.B.; Yu, A.B.; Vince, A.; Barnett, G.D.; Barnett, P.J. Prediction of wear and its effect on the multiphase flow and separation performance of dense medium cyclone. *Miner. Eng.* **2014**, *56*, 91–101. [CrossRef]
12. Bu, X.; Ni, C.; Xie, G.; Peng, Y.; Ge, L.; Sha, J. Preliminary study on foreign slime for the gravity separation of coarse coal particles in a teeter bed separator. *Int. J. Miner. Process.* **2017**, *160*, 76–80. [CrossRef]
13. Galvin, K.P.; Pratten, S.J.; Lambert, N.; Callen, A.M.; Lui, J. Influence of a jigging action on the gravity separation achieved in a teetered bed separator. *Miner. Eng.* **2002**, *15*, 1199–1202. [CrossRef]
14. Sumer, B.M.; Fredsøe, J.; Christensen, S.; Lind, M.T. Sinking/floatation of pipelines and other objects in liquefied soil under waves. *Coast. Eng.* **1999**, *38*, 53–90. [CrossRef]
15. Ren, D.; Yang, Y.; Yang, Y.; Richards, K.; Zhou, X. Land-Water-Food Nexus and indications of crop adjustment for water shortage solution. *Sci. Total Environ.* **2018**, *626*, 11–21. [CrossRef]
16. Mohanta, S.; Rao, C.S.; Daram, A.B.; Chakraborty, S.; Meikap, B.C. Air Dense Medium Fluidized Bed for Dry Beneficiation of Coal: Technological Challenges for Future. *Part. Sci. Technol.* **2013**, *31*, 16–27. [CrossRef]
17. Sahu, A.K.; Parida, S.K.B.; Parida, A. Development of Air Dense Medium Fluidized Bed Technology For Dry Beneficiation of Coal—A Review. *Int. J. Coal Prep. Util.* **2009**, *29*, 216–241. [CrossRef]
18. Luo, Z.F.; Chen, Q.R. Dry beneficiation technology of coal with an air dense-medium fluidized bed. *Int. J. Miner. Process.* **2001**, *63*, 167–175.
19. Luo, Z.; Zhao, Y.; Yu, X.; Duan, C.; Song, S.; Yang, X. Effects of characteristics of clapboard unit on separation of <6 mm fine coal in a compound dry separator. *Powder Technol.* **2017**, *321*, 232–241. [CrossRef]
20. Yu, X.; Luo, Z.; Li, H.; Gan, D. Effect of vibration on the separation efficiency of oil shale in a compound dry separator. *Fuel* **2018**, *214*, 242–253. [CrossRef]
21. Boylu, F.; Tali, E.; Cetinel, T.; Celik, M.S. Effect of fluidizing characteristics on upgrading of lignitic coals in gravity based air jig. *Int. J. Miner. Process.* **2014**, *129*, 27–35. [CrossRef]
22. Breuer, H.; Snoby, R.J.; Mshra, S.; Biswal, D. Dry coal jigging—A suitable alternative for Indian power coals. *J. Mines Met. Fuels* **2009**, *57*, 425–428.
23. Yang, X.; Fu, Z.; Zhao, J.; Zhou, E.; Zhao, Y. Process analysis of fine coal preparation using a vibrated gas-fluidized bed. *Powder Technol.* **2015**, *279*, 18–23. [CrossRef]
24. Yang, X.L.; Fu, Z.J.; Zhao, Y.M. Slugging Behavior of Geldart D Particles in a Vibrated Gas-Fluidized Bed. *Part. Sci. Technol.* **2014**, *32*, 537–543. [CrossRef]
25. Yang, X.L.; Zhao, Y.M.; Luo, Z.F.; Song, S.L.; Duan, C.L.; Dong, L. Fine coal dry cleaning using a vibrated gas-fluidized bed. *Fuel Process. Technol.* **2013**, *106*, 338–343. [CrossRef]
26. Luo, Z.F.; Zhao, Y.M.; Chen, Q.R.; Fan, M.M.; Tao, X.X. Separation characteristics for fine coal of the magnetically fluidized bed. *Fuel Process. Technol.* **2002**, *79*, 63–69. [CrossRef]
27. Hao, B.G.; Bi, H.T. Forced bed mass oscillations in gas-solid fluidized beds. *Powder Technol.* **2005**, *149*, 51–60. [CrossRef]
28. Saidi, M.; Tabrizi, H.B.; Grace, J.R.; Lim, C.J.; Ahmad, G. Hydrodynamic and Mixing Characteristics of Gas-Solid Flow in a Pulsed Spouted Bed. *Ind. Eng. Chem. Res.* **2015**, *54*, 7933–7941. [CrossRef]
29. Zhao, Y.; Li, G.; Luo, Z.; Zhang, B.; Dong, L.; Liang, C.; Duan, C. Industrial Application of a Modularized Dry-Coal-Beneficiation Technique Based on a Novel Air Dense Medium Fluidized Bed. *Int. J. Coal Prep. Util.* **2017**, *37*, 44–57. [CrossRef]
30. Geldart, D. Types of gas fluidization. *Powder Technol.* **1973**, *7*, 285–292. [CrossRef]
31. Zhou, C.; Dong, L.; Zhao, Y.; Fan, X. Studies on Bed Density in a Gas-Vibro Fluidized Bed for Coal Cleaning. *ACS Omega* **2019**, *4*, 12817–12826. [CrossRef]
32. Fan, X.; Zhou, C.; Zhao, Y.; Duan, C.; Liu, Q. Flow pattern transition and coal beneficiation in gas solid fluidized bed with novel secondary distributor. *Adv. Powder Technol.* **2018**, *29*, 1255–1264. [CrossRef]
33. Fan, X.C.; Zhou, C.Y.; Dong, L.; Zhao, Y.M.; Duan, C.L.; Zhang, B. Novel method of air distributor design for enhancing bed stability and reducing impurities in gas-solid fluidized bed system. *Part. Sci. Technol.* **2019**, *37*, 652–664. [CrossRef]
34. Geldart, D. *Gas Fluidization Technology*; John Wiley and Sons Inc.: New York, NY, USA, 1986. Available online: https://www.osti.gov/biblio/6808024 (accessed on 8 December 2021).
35. Li, G.; Liu, X.; Duan, C.; Liu, Q.; Zhao, Y.; Gupta, R. Study on the spatial and temporal distribution of the bed density in an air dense medium fluidized bed (ADMFB) based on the electrical capacitance tomography (ECT) measurement system. *Powder Technol.* **2021**, *393*, 659–669. [CrossRef]
36. Liu, X.; Fan, X.; Zhao, Y.; Duan, C.; Zhou, C. Particles movement behavior and apparent density in gas–solid fluidized bed as determined by an electronic dynamometer and electrical capacitance tomography. *Chem. Eng. J.* **2022**, *429*, 132463. [CrossRef]
37. Zhou, E.; Zhang, Y.; Zhao, Y.; Tian, Q.; Chen, Z.; lv, G.; Yang, X.; Dong, L.; Duan, C. Influence of bubbles on the segregated stability of fine coal in a vibrated dense medium gas–solid fluidized bed. *Particuology* **2021**, *58*, 259–267. [CrossRef]
38. Matheson, G.L.; Herbst, W.A.; Holt, P.H. Characteristics of Fluid-Solid Systems. *Ind. Eng. Chem.* **1949**, *41*, 1098–1104. [CrossRef]
39. Bertil Andersson, K.E. Pressure drop in ideal fluidization. *Chem. Eng. Sci.* **1961**, *15*, 276–297. [CrossRef]
40. Pyle, D.L.; Harrison, D. The rising velocity of bubbles in two-dimensional fluidised beds. *Chem. Eng. Sci.* **1967**, *22*, 531–535. [CrossRef]

41. Toomey, R.D.; Johnstone, H.F. Gaseous fluidization of solid particles. *Chem. Eng. Prog.* **1952**, *48*, 220–225.
42. Asthana, H.; Sarkar, S. Coal cleaning in fluidized bed. *Chem. Ages India* **1969**, *20*, 792–796.
43. Peters, M.H.; Fan, L.-S.; Sweeney, T.L. Reactant dynamics in catalytic fluidized bed reactors with flow reversal of gas in the emulsion phaset. *Chem. Eng. Sci.* **1982**, *37*, 553–565. [CrossRef]
44. Davidson, J.F.; Harrison, D.; Jackson, R. Fluidized particles: Cambridge University Press, 1963. 155 pp. 35s. *Chem. Eng. Sci.* **1964**, *19*, 701. [CrossRef]
45. Darton, R.C.; Lanauze, R.D.; Davidson, J.F.; Harrison, D. Bubble Growth Due To Coalescence in Fluidized Beds. *Trans. Inst. Chem. Eng.* **1977**, *55*, 274–280.